Clim. Past, 22, 1741–1756, 2026
https://doi.org/10.5194/cp-22-1741-2026

Climate of the Past
Open Access

Trends in south pole particle concentrations imply holocene westerly wind strengthening

Aaron Chesler[1,2,a], **Dominic Winski**[1,2], **Karl Kreutz**[1,2], **Bess Koffman**[3], **Erich Osterberg**[4], **David Ferris**[4], **Zayta Thundercloud**[4], **Jihong Cole-Dai**[5], **Mark Wells**[6], **Aaron Putnam**[2], **and Katherine Anderson**[4]

[1]Climate Change Institute, University of Maine, Orono, Maine, 04469, USA
[2]School of Earth and Climate Sciences, University of Maine, Orono, Maine, 04469, USA
[3]Department of Geology, Colby College, Waterville, Maine, 04903, USA
[4]Department of Earth Science, Dartmouth College, Hanover, New Hampshire, 03755, USA
[5]Department of Chemistry and Biochemistry, South Dakota State University, Brookings, South Dakota, 57007
[6]School of Marine Sciences, University of Maine, Orono, Maine, 04469, USA
[a]now at: Environmental Studies and Science Program, Colorado College, Colorado Springs, 80903, USA

Correspondence: Aaron Chesler (aaron.chesler@maine.edu)

Received: 22 April 2025 – Discussion started: 8 May 2025
Revised: 17 April 2026 – Accepted: 30 April 2026 – Published: 28 September 2026

Abstract. The Southern Hemisphere Westerly Winds (SHWW) play an important role in global climate and Antarctic ice sheet dynamics; however, high-resolution proxy reconstructions are sparse. Conflicting evidence suggests SHWW latitudinal change, weakening and/or strengthening, throughout the Holocene. Dust microparticle characteristics preserved in Antarctic ice cores (i.e., changes in concentration and size) provide a useful physical proxy reflecting wind dynamics. We present South Pole Ice Core (SPC14) dust records spanning the Holocene. Dust concentrations (1.1–5.1 µm) decrease through the Holocene, while the coarse particle percentage (CPP) increase due to a relatively larger decrease in finer (1.1–3.2 µm) dust, highlighting an opposing trend. The South Pole dust trends, consistent with CMIP6-PMIP4 model trends, southern mid-latitude insolation, and mid- to high latitude Southern Hemisphere proxy records, reflect SHWW southward migration and strengthening of wind speed south of 51° S during the mid-Holocene (∼ 7000–3000 years ago). Our findings suggest orbitally-driven warming throughout the Holocene led to strengthening and southward migration of the SHWW beginning ∼ 7000 years BP.

1 Introduction

The Southern Hemisphere Westerly Winds (SHWW) represent the strongest persistent surface wind system on Earth. Variations in the SHWW influence global carbon cycling and heat distribution, and are believed to play a critical role in Earth's climate and ice sheet stability across wide-ranging timescales (Hillenbrand et al., 2017; Russell et al., 2006). Variations of the strength and latitudinal position of the SHWW during the past several centuries are related to changes in the equator-to-pole temperature gradient (i.e., Perren et al., 2020). During warm periods, SHWW migrate southward and increase in strength and during cooler periods migrate northward and weaken. Increases in SHWW strength intensify the ocean-to-atmosphere transfer of CO_2 via upwelling and impact ice sheet stability and mid-latitude vegetation/precipitation dynamics (Hillenbrand et al., 2017; Anderson et al., 2009; Toggweiler and Russell, 2008; Moreno et al., 2010).

However, while the SHWW are an important climatic feature, complete Holocene SHWW dynamics are poorly constrained. Previous research has focused on three possibilities for the style of change; (1) strong southward SHWW displacement at the start of the Holocene and northward displacement with cooling and/or stable temperatures beginning ∼ 9–7.5 ka (Hillenbrand et al., 2017; Kaplan et al., 2016;

Mulvaney et al., 2012), (2) progressive strengthening and southward displacement of the SHWW between ∼ 8–7 ka (Moreno et al., 2010; Saunders et al., 2018; Zwier et al., 2022), and (3) strengthening of the SHWW wind belt core with latitudinal contraction of the northern margin of the winds throughout the past 12 ka (Lamy et al., 2010). Furthermore, the early Holocene is hypothesized to be a climatically similar period to the present day, facilitating comparison to ongoing climate dynamics (Marcott et al., 2013; Kaufman et al., 2020). However, Osman et al. (2021) provides an alternative scenario, with global average temperature steadily increasing throughout the Holocene, which suggests that the Early Holocene would not be a comparable period for comparison to modern climate dynamics. The current ambiguity of Holocene and in particular early Holocene SHWW dynamics is critical for understanding West Antarctic Ice Sheet (WAIS) stability and future climate projections (i.e., Bronselaer et al., 2020).

Records of microparticle concentration and relative particle size (i.e., coarse particle percentage; CPP) from Antarctic ice cores offer a unique perspective on SHWW strength and/or position dynamics because they have been interpreted to reflect source-to-sink conditions and atmospheric variability, specifically distillation (Markle et al., 2018), geomorphology of the source regions (Sugden et al., 2009), wind strength (Koffman et al., 2014), vegetation cover, precipitation (Tegen and Schepanski, 2018), and atmospheric transport patterns (Albani et al., 2018; Delmonte et al., 2020, 2013, 2002; Aarons et al., 2019, 2017, 2016; Koffman et al., 2023). Holocene dust records differ among Antarctica ice cores, with East Antarctic Plateau data reflecting atmospheric subsidence and peripheral cores reflecting regional variability (Delmonte et al., 2020; Albani et al., 2012). The relative few complete and available Holocene dust records from Antarctica prevent a full interpretation of past SHWW behavior.

The South Pole is well-situated for Southern Hemisphere atmospheric reconstructions because (1) the symmetric position with respect to the annular SHWW belt favors interpretation of the hemispheric, rather than regional, SHWW system, (2) the relatively high snow accumulation rate (8 cm w.e. a^{-1}) relative to other sites in East Antarctica provides strong constraints on the ice core chronology and high temporal resolution and (3) aerosol and meteorological studies have been conducted at this location over the past 60 years, which provides context for paleo-interpretations (Lazzara et al., 2012; Sheridan et al., 2016; Clem et al., 2020; Casey et al., 2014). The South Pole primarily receives aerosols during the austral summer (DJF) via air masses moving into the East Antarctic plateau, most prominently via the Weddell Sea and the Amundsen-Bellingshausen Sea embayment (Nicolas and Bromwich, 2011; Lazzara et al., 2012; Clem et al., 2020; Tuncel et al., 1989). South Pole aerosols and particulates (i.e., cloud condensation nuclei and dust particles) are sensitive to seasonal and synoptic variability over the past 40 years, demonstrating that trends in ice-core particle records likely reflect long-term climate variability (Hogan et al., 1984; Parungo et al., 1981; Ardon-Dryer et al., 2011; Sheridan et al., 2016). We build upon instrumental-era South Pole particle research to investigate particle variability on centennial to millennial scales throughout the Holocene using dust records from the new SPC14 intermediate-depth ice core to better constrain SHWW dynamics within the context of early Holocene to modern climate dynamics.

2 Methods

Microparticle concentrations and size distributions were measured with a Klotz Abakus laser dust sensor on a continuous flow analysis (CFA) system at Dartmouth College (Sect. S1 in the Supplement; Breton et al., 2012; Winski et al., 2021; Osterberg et al., 2006). We use a subset (size 1.1–5.1 µm) of the particle data and focus our data analysis on the period from 11 300 to 250 years BP based on particle size distributions (Fig. 1). Uncertainty in the SPC14 age model during the Holocene is ±18 years while between 1800–3100 years BP the uncertainty increases to ±25 years (Winski et al., 2019). While the CFA can produce data with nominal sub-annual resolution, we resample the dust data yielding the median value in 50-year intervals.

To facilitate a comparison with other ice core records, we assume a spherical particle shape, rather than the measured prolate particle shapes (Chesler et al., 2023), use a density of 2.6 g cm^{-3} (following Koffman et al., 2014) to estimate particle mass flux, and, when possible, restrict particle flux to similar size ranges (1.1–5.1 µm; Figs. 1e and 2). South Pole particle shape metrics (i.e., mass and flux) are unconstrained for the Holocene because of limited data (i.e., Chesler et al., 2023). In previously published ice core dust records using solely laser particle measurement techniques, the particle shape has been assumed to be spherical (Chesler et al., 2023; Simonsen et al., 2018; Potenza et al., 2016). Studies concerned with the absolute magnitude of dust flux at the South Pole should use prolate particle shapes to calculate flux (Chesler et al., 2023; data at USAP-DC, https://doi.org/10.15784/601553, Kreutz, 2022). We restrict particle metrics to number concentration and CPP because the particle shape assumption (i.e., particle flux and mass concentration), can artificially increase particle metric concentrations by 25 %–44 %. While this produces higher-than-realistic particle flux values, it mitigates discrepancies from comparing records with dissimilar metrics.

We use particle number concentration measured between 1.1–5.1 µm and CPP (defined as number of particles mL^{-1} [3.2–5.1] / [1.1–5.1] µm diameter ×100; Fig. 1) following other East Antarctic studies due to the similarity of the South Pole particle flux to other East Antarctic ice core records (Fig. 2a and b; i.e., Delmonte et al., 2020). To avoid spurious correlation of ratios between our analyses, we also compare the coarse particle fraction (3.2–5.1 µm # particles mL^{-1}) to our fine particle fraction (1.1–3.2 µm # mL^{-1}), which we refer to as our coarse:fine ratio (CFR). Our CPP and CFR have a significantly strong relationship ($r = 0.95$, p-value = < 0.01), suggesting similar forcings behind these particle size metrics.

HYSPLIT and CMIP6-PMIP4 models

We obtain HYSPLIT NCEP trajectories for December, January, February (austral summer; DJF) and June, July, August (austral winter; JJA) from 1980–2022 (inclusive) hourly for 10 d over a 90 d period. We run the model at an altitude of 1000 m following Schwanck et al. (2017) and use the default vertical motion for the model. We then calculate air mass origin percentage using a 2×2° grid to identify where air masses originate 10 d prior to reaching the South Pole.

We also explore changes in atmospheric temperature, wind speed, and precipitation using CMIP6–PIMP4 model outputs. We use 11 different models (Table 1) to assess model agreement between mid-Holocene runs (6000 years ago) relative to pre-industrial control (piControl). We calculate model difference by subtracting the mid-Holocene from pre-industrial to assess change in each climate variable from the mid-Holocene to the pre-Industrial. We replace all positive values with a value of 1, which signifies an increase with time, and replace all negative values with a 0 and sum all model runs. Our method allows us to assess if the models agree to an increase/decrease in each climate variable rather than assessing the magnitude of change between each model. We test statistical significance by selecting data in the mid-Holocene and piControl runs using a 10 × 10° grid. We use a t-test to identify significant difference between the two periods for each model run (p-value < 0.05). If the two periods are significantly different, then replace the values with a 1 and sum the totals between models, similar to our model agreement analysis.

3 Results

South Pole dust concentration decreases during the mid-Holocene (∼ 7000–3000 years BP) compared to the relatively stable early Holocene (11 300–7000 years BP), and a moderate decrease in the late Holocene (3000–250 years BP). The rate of the concentration decrease during the mid-Holocene is double that of the late Holocene and coincides with an increase in the CFR and CPP (Fig. 1a–c). South Pole particle flux and NOAA HYSPLIT analysis suggests that trends in the South Pole particle flux are similar to those in other Antarctic records (Fig. 2a and b) and broadly reflects synoptic scale Antarctic climate (Fig. 3a and b). Therefore, we suggest the South Pole particle trends are reflective of Holocene mid-high latitude synoptic climate variability.

Table 1. List of CMIP6-PMIP4 Models used with name, institution, resolution using the r1i1p1 (r = realization, i = initialization, p = physics, respectively) ensemble, with variables for surface temperature (tas), precipitation, (pr), and surface wind speed (sfc Wind). All data was downloaded using the atmospheric monthly data (Amon) time resolution.

Model	Institute	Grid Size		Model Run Time		Variables
		Latitude (°)	Longitude (°)	mid-Holocene	piControl	
ACCESS-ESM 1-5	Commonwealth Scientific and Industrial Research Organization, Australia	1.25	1.88	501–800	101–0600	pr, tas
AWI-ESM-1-1-LR	Alfred Wegner Institute, Germany	1.85	1.88	3106–3205	1850–1954	pr, sfcWind, tas
FGOALS-f3-L	Chinese Academy of Sciences, China	1	1.25	720–1219	600–1160	pr, sfcWind, tas
GISS-E2-1-G	Goddard Institute for Space Studies, USA	2	2.5	2900–3199	4150–5000	pr, sfcWind, tas
INM-CM4-8	Institute for Numerical Mathematics, Russian Academy of Science, Russia	1.5	2	1880–2079	1850–2380	pr, sfcWind, tas
IPSL-CM6A-LR	L'Institut Pierre-Simon Laplace, France	1.27	2.5	1850–2399	1850–2349	pr, sfcWind, tas
MPI-ESM1-2-LR	Max Planck Institute for Meteorology, Germany	1.85	1.88	1001–1500	1850–2849	sfcWind
MRI-ESM2-0	Meteorlogical Research Institute, Japan	1.11	1.13	1951–2150	1850–2550	pr, sfcWind, tas
NCAR – CESM2	National Center for Atmospheric Research, USA	0.94	1.25	0–700	1–1200	pr, sfcWind, tas
NUIST – NESM3	Nanjing University of Information Science and Technology, China	1.875	1.875	1798–1897	500–0999	pr, tas
NorESM2-LM	Norwegian Climate Centre	1.875	2.5	2101–2200	1600–2100	pr, tas

3.1 Holocene trends in dust deposited at the South Pole

The number concentrations of particles in the size range 1.1–5.1 µm comprise on average ∼ 85 %–96 % of all particles measured (median $\pm 1\sigma$; Fig. 1a and b). The total dust number concentration and CPP (Fig. 1a–c) abundance have opposing trends, yet the timing of change in both trends begins about ∼ 7000 years BP. This inverse relationship is most apparent during the mid-Holocene (∼ 7000–3000 years BP). Because trend changes occur around the mid-Holocene, we divide the Holocene into early (11 300–7000 years BP), middle (7000–3000 years BP) and late (3000–250 years BP) periods. During the early Holocene, dust concentration remained relatively stable (∼ −1.7 particles mL^{-1} kyr^{-1}) followed by a significant decrease (∼ −50 particles mL^{-1} kyr^{-1}) until the Late Holocene where particle concentrations continued to decrease but at half the rate of the mid-Holocene (∼ 24 particles mL^{-1} yr^{-1}; Table S1). Dust concentration distributions in all three time periods are statistically different (Fig. 1d; p-value < 0.01; Table S2a), further indicating a significant reduction in Holocene dust deposition. During the mid-Holocene, there is a bimodal distribution highlighting the transition from early to late Holocene (Fig. 1d). During the early and late Holocene, the dust concentration is more normally distributed.

The number concentration of coarse particles (Fig. 1b) has a decrease similar to the total particle concentration (Fig. 1a), but the coarse particle decrease is an order of magnitude smaller (∼ −4 # particles mL^{-1} kyr^{-1}) during the mid-Holocene. The decrease in total dust concentration from the Early Holocene to Late Holocene is about 40 % and about 35 % for coarse dust concentration. This 5 % difference results in an increase in the CPP starting at ∼ 7000 years BP, where over the Holocene, CPP significantly increases from 8.6 % to 9.4 % (two-sided t-test; p-value < 0.01; Table S2b). Although the coarse dust concentration also decreases slightly throughout the Holocene, the decrease is much less than that of the total dust concentration slope such that the proportion of coarse particles rises, especially during the middle Holocene. CPP has a weak statistical relationship with dust concentration during the Holocene (Spearman $r = -0.28$; $p < 0.01$), suggesting that their variability may be driven by different and/or independent factors. Because total dust concentration was used in the creation of the CPP metric, we test this relationship with CFR and identify a statistically weaker relationship ($r = -0.15$, $p < 0.05$). The statistically weaker relationship further supports the above interpretation of independent factors driving their variability.

3.2 Holocene dust flux

South Pole Holocene dust flux (0.45 ± 0.23 mg m^{-2} yr^{-1}; 2σ; 50-year resampled) has a similar magnitude and trend to other East Antarctic Plateau ice core sites (Fig. 2a; following Koffman and Kreutz, 2014). The SPC14 Holocene median dust flux is within 2σ of the EPICA Dome C (0.33 ± 0.23) and Vostok dust flux records (0.63 ± 0.21), while non-plateau sites (i.e., TALDICE [∼ 1.31 mg m^{-2} yr^{-1}] and WAIS Divide [∼ 1.36 mg m^{-2} yr^{-1}; particles < 5.1 µm]) are significantly higher (Fig. 2b; Koffman et al., 2014; Albani et al., 2012; Lambert et al., 2012; Petit et al., 1990).

Following Albani et al. (2012), we compare our Holocene dust flux record against $\delta^{18}O$, a proxy for local atmospheric air temperature, to assess whether there are primarily remote or mixed dust source (Steig et al., 2021). Albani et al. (2012) compared the TALDICE dust-$\delta^{18}O$ profile against EPICA Dome C as EPICA Dome C is considered to represent remote dust sources. We define remote dust sources similarly, as those from the mid-latitudes (i.e., southern South America and Australia; Delmonte et al., 2020), local sources from Antarctica (i.e., Aarons et al., 2019), and mixed being a combination of the remote and local. The Holocene South Pole dust record and $\delta^{18}O$ have a weak, albeit significant relationship ($r = -0.17$, $p =< 0.01$; Fig. 2b), which suggests a primarily remote dust source signal. Albani et al. (2012) interpreted the close relationship between dust and $\delta^{18}O$ trends at Talos Dome as evidence of a local/regional climate influence. Conversely at Dome C during the Holocene, the dust and $\delta^{18}O$ did not vary coevally, which is interpreted to reflect mid-to-high latitudinal processes (Lambert et al., 2008; Albani et al., 2012).

3.3 Modern air mass sources

Our NOAA HYSPLIT results from austral summer (DJF) and winter (JJA; 1980–2022) both highlight a dominant Atlantic sector signal (Fig. 3; Rolph et al., 2017; Stein et al., 2015). Austral summer air masses at their 10 d origin are from the Weddell Sea, Dronning Maud Land, Enderby and Kemp Land (i.e., Atlantic Sector; Fig. 3a), while austral winter air masses origins are more latitudinally and longitudinally diverse, with a greater percentage of air mass originates from the Atlantic and Pacific sectors of the Southern Ocean (Fig. 3b). While both the longitude and latitude seasonal origins differ, the change is most pronounced in the latitudinal variability (Fig. 3c and d). A primary austral summer peak was observed in previous South Pole dust and meteorological records (Lazzara et al., 2012; Carrasco et al., 2003; Parungo et al., 1981; Hogan et al., 1984; Bodhaine et al., 1986). Our HYSPLIT analysis identifies DJF 10 d air mass origin locations with an average coordinate of 70.9 (±9.4)° S, −1.4 (±80.03)° W, indicating a primarily Weddell Sea/Atlantic Sector modern signal. The similarity results from other East Antarctica sites (i.e., Dome C and Vostok; Fig. 2b), the modern back-trajectory modelling (Fig. 3), and the dust-water isotopes relationships all suggest that South Pole represents a site typical of Antarctic plateau locations, with the majority

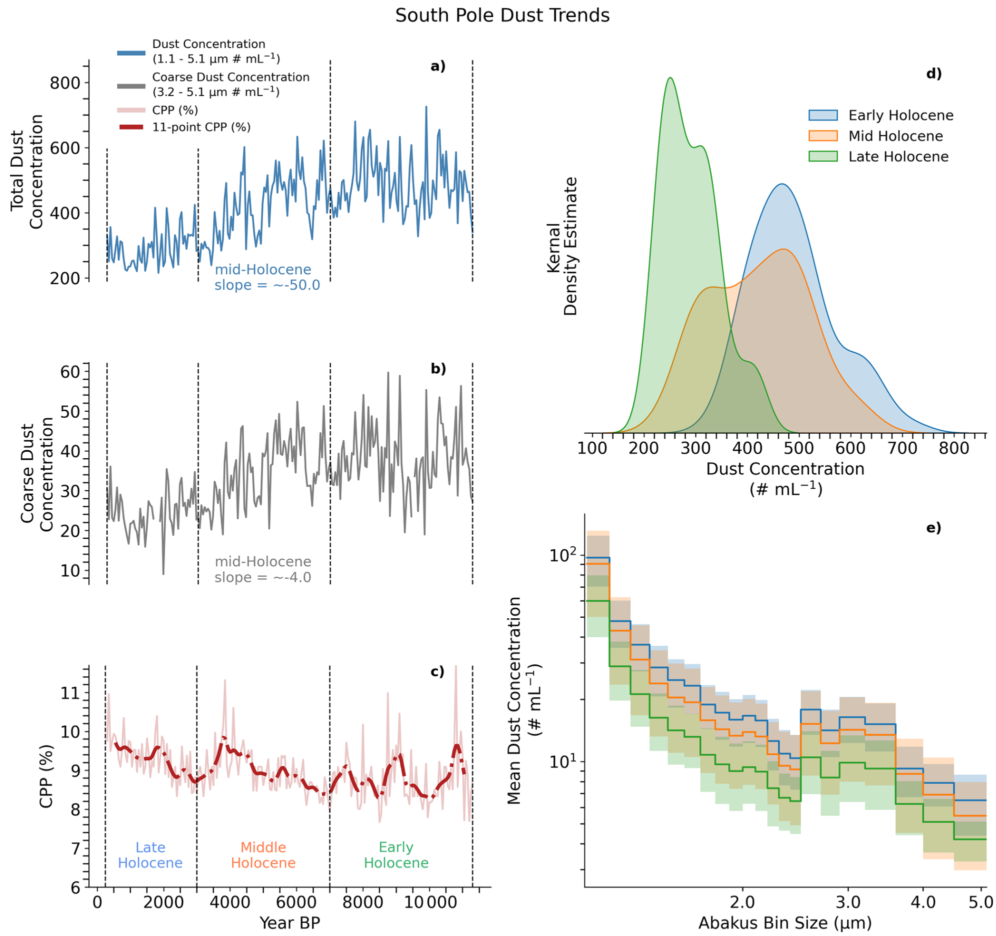

Figure 1. **(a)** 50-year median resampled SPC14 total dust concentration (1.1–5.1 µm # particles mL^{-1}; blue line), **(b)** 50-year median resampled coarse particle concentration (3.2–5.1 µm # particles mL^{-1}; grey line), **(c)** 50-year median resampled CPP (light red) and CPP 11-point rolling gaussian mean (2σ; red dashed line), **(d)** total dust # particles mL^{-1} concentration distributions, and **(e)** total dust # particles mL^{-1} size distributions by time period. Average median absolute deviation (MAD) for the particle concentration is $\sim$84 (Fig. S1). Mid-Holocene slopes values are reported in # particles mL^{-1} kyr^{-1}.

of dust likely sourced from remote regions rather than mixed remote-local dust sources, facilitating comparisons (Fig. 2).

4 Discussion

We interpret the opposing South Pole particle trends and metrics to reflect strengthening and southward migration of the SHWW throughout the Holocene. We reach these conclusions based on a predominantly southern South American and Antarctic dust source regions through terrestrial and oceanographic paleoproxy records and PMIP4-CMIP6 atmospheric modelling analyses. Our interpretations suggest that insolation-like southern hemisphere warming throughout the Holocene lead to increasing wind strength and southward migration. Based on our interpretations, our data suggests that the early Holocene may not be a climatically comparable period to modern climate, and that Southern Hemisphere temperatures have increased throughout the Holocene.

4.1 Dust source(s)

The South Pole receives air masses from multiple different Antarctic regions, including Western Antarctica (Nicolas and Bromwich, 2011), the Weddell Sea (Winski et al., 2021; Lazzara et al., 2012; Arimoto et al., 2008), and downslope from the East Antarctic Plateau (Lazzara et al., 2012). The dominant advection of remote air masses are from Weddell Sea and WAIS with a minor source from EAIS (Harris, 1992). Our HYSPLIT data analysis then is reflective of past studies and highlights modern seasonal latitudinal changes in wind strength and position of 10 d air mass origins. While we recognize that some air masses and dust particles can be sourced from the East Antarctic Plateau, this area would not be the primary source of reduced dust emission during the mid-Holocene since southern South America and Australia are the primary sources of dust during the Holocene and modern period (Wegner et al., 2012; Vecchio et al., 2024; Delmonte et al., 2020). Given the multiple trajectories of air masses to

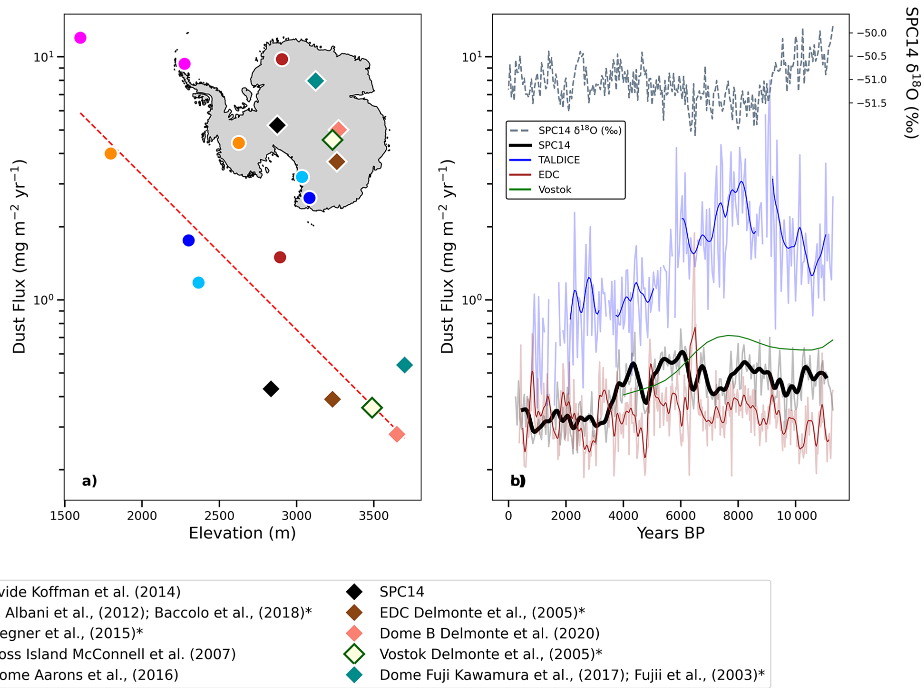

Figure 2. Comparison of SPC14 dust metrics with other Antarctic Holocene records. In **(a)**, SPC14 dust flux is similar to other cores based on drill site elevation (following Koffman and Kreutz, 2014). Plateau sites are depicted with diamonds while non-plateau (i.e., WAIS and coastal locations) are depicted with circles. Labels containing * symbol at the end were reported in (Delmonte et al., 2020). **(b)** South Pole (SPC14) and δ^{18}O (Steig et al., 2021) resolved to 50-year resolution shows available Holocene flux records from Talos Dome fine (0.6–5 µm mg m^{-2} yr^{-1}; Albani et al., 2012), Vostok (Petit et al., 1990), EPICA Dome C (EDC; Lambert et al., 2012). SPC14 dust flux is similar to other East Antarctic sites (Vostok and EDC) and is on average ∼ 67 % lower compared to TALDICE. TALDICE, SPC14, and EDC were resampled to 50-year median values (background variability), and the darkened lines are the 11-point rolling gaussian mean for TALDICE, SPC14, and EDC. WAIS Divide (Koffman et al., 2014), James Ross Island (McConnell et al., 2007), and SPC14 dust fluxes (this study) were measured using a laser particle counter and Dome Fuji (Fujii et al., 2003; Dome Fuji Ice Core Project Members et al., 2017) was measured using both light scattering techniques and a laser particle counter. All other records were measured using a Coulter Counter providing volume accurate measurements (Baccolo et al., 2018; Albani et al., 2012; Delmonte et al., 2020, 2013, 2005; Aarons et al., 2016).

the South Pole, we do not specify a specific dust source contributor but rather limit our interpretation to local or remote dust sources.

4.2 Proxy and modelled Holocene wind changes

We suggest that the SPC14 dust concentration and CPP records indicate a mid-to-high latitude (> ∼ 51° S) strengthening and southward shift of the SHWW during the mid-Holocene (∼ 7000–3000 years BP), consistent with other proxy-based reconstructions of SHWW migration and CMIP6-PMIP4 model output (Fig. 4). Simulations from an ensemble of CMIP6-PMIP4 models (Table 1; Fig. 4b), all show a clear pattern of decreased and significant surface wind strength over South American and mid-latitude (40–50°) oceans concurrent with increasing surface wind strength over the Antarctic periphery between the mid-Holocene (6000 BP) and pre-Industrial (piControl; Fig. 4b and e). The weakening of the SHWW over lower latitudes < ∼ 51° S is consistent with the observed decrease in the SPC14 dust concentration, indicating a reduced entrainment of fine remote dust sources in surface winds. We note broad agreement spatially with Southern Hemisphere temperature and precipitation increase between the mid-Holocene and pre-Industrial periods over common dust source regions (i.e., South America, Australia, and Antarctica; Fig. 4a, c, e, and f). A southward shift in the core of the SHWW can simultaneously explain the opposing trends in CPP and total particle concentration at the South Pole while being consistent with proxy records reflecting changes in winds, precipitation and/or glacier retreat across the mid-to-high-latitude Southern Hemisphere during the mid-Holocene.

More northern proxy records corroborate a poleward shift in the SHWW during the mid-Holocene. Lacustrine sediments from Emerald Lake, Macquarie Island (∼ 55° S, ∼ 159° E) reflect a weakening of the SHWW between 11 200–9200 years BP, followed by a period of increased variability between 9200–5300 years BP, and sustained and strengthened winds between 5300–200 years BP (Fig. 5f; Saunders et al., 2018). In southern South America, Moreno et

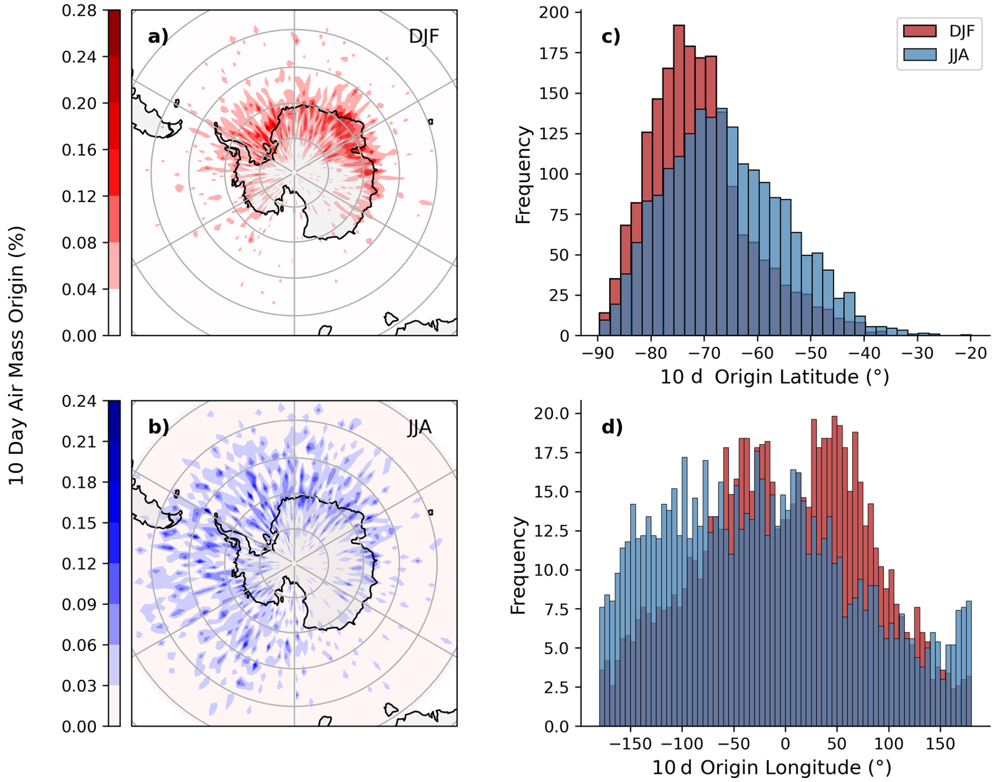

Figure 3. NOAA HYSPLIT analysis of 10 d hourly back-trajectory of air masses to the South Pole from 1980–2020 (Rolph et al., 2017; Stein et al., 2015). Height elevation of back trajectory is 1000 m. **(a)** and **(b)** indicate the percentage of 10 d air masses (240 h) in a 2 × 2° grid. **(c)** and **(d)** are histograms of frequency of seasonal data by latitude and longitude, respectively.

al. (2010) also suggested a progressive southward shift in the SHWW, which they interpreted from precipitation dynamics via plant community changes beginning ∼ 7800 years BP (Fig. 5e; Lago Guanaco and Lago Condorito; 51° [Fig. 5e] and 41° S, respectively, ∼ 72° W). We discuss the impact of precipitation changes in Sect. 4.3. These changes were interpreted to reflect a relatively weak SHWW influence during the Early Holocene followed by a strengthening of the SHWW influence during the middle and late Holocene, which is consistent with Saunders et al. (2018; Fig. 5f).

The timing of inferred changes in the SHWW are not zonally consistent, suggesting regional variability. In the eastern Pacific Ocean in New Zealand (43° S, 171° E), progressive glacier retreat and southward shift in the ITCZ and SHWW occur between ∼ 9800 and ∼ 6900 years ago, suggesting a warming early Holocene (Fig. 5c; Putnam et al., 2012). Whereas in South America, the changes located at Lago Condorito and Lago Guanaco suggest southward migration starting at the earliest at 7800 years ago (Fig. 5e; Moreno et al., 2010). While southern South America might suggest a relatively linear change in the SHWW (Fig. 5e) this does not negate a non-linear shift in the SHWW belt in other regions. The offset between these two records would suggest zonal variability across the Pacific, in agreement with Kaplan et al. (2016).

The regional inconsistency is reflected in the global mean surface temperature (GMST) reconstruction in Osman et al. (2021). We also compare our total dust number concentration results using the GMST reconstruction record throughout the Holocene (11 300–100 years ago) from the Western and Eastern Pacific Ocean 30–55° S similarly to Lamy et al. (2010) to assess temperature (wind) gradients (Fig. S2). We find that average temperature gradients steepen, which we interpret to reflect a strengthening of the winds throughout the Holocene. Statistically, the dust concentration record has a significant anticorrelating relationship to both temperature gradients (p-value < 0.01) for both the western and eastern mid-latitudinal Pacific Ocean. However, the South Pole dust concentration has a stronger anticorrelating relationship to the western Pacific Ocean compared to the eastern Pacific Ocean ($r = -0.76$ and -0.65, respectively). We interpret this relationship to reflect changes in the Westerly Winds shifts and warm water circulation into the south Pacific gyre, which was also hypothesized by Denton et al. (2021) to explain the onset of mountain glacier retreat during Termination I. Similar atmospheric dynamics may also occur during the Holocene. Furthermore, regional asymmetry in the SHWW can explain our record of a southward shift and strengthening of the winds and cooling of coastal South American temperatures throughout the Holocene (Lamy et al., 2010; Kaplan et al., 2016), and upwelling in Pine Island Bay during the early Holocene (Fig. 5g; Hillenbrand et al., 2017).

Our interpretation of SHWW southward shift during the Holocene should correspond with changes in precipitation. Koffman et al. (2014) used Patagonian and Southern South American precipitation records in conjunction with WAIS Divide dust particle records to infer wind changes. Although the South Pole dust records are consistent with a southward shift in the SHWW, a corresponding increase in precipitation would further suggest such a change throughout the Holocene, rather than a possible decrease in glacial activity and/or vegetation change. Therefore, we assess our inferred dynamics of the SHWW within the context of precipitation variability over the Southern Hemisphere.

4.3 Changes in SPC14 dust concentration and hydrologic conditions

From 7000–3000 years BP, South Pole dust concentration decreased by ∼ 40 % (Table S1). While we have shown this decrease is qualitatively consistent with a reduction in Patagonian surface winds, possibly related to SHWW variability (<∼ 51° S; Fig. 5a), increased precipitation in the remote dust source regions (Figs. 4 and 5d and e; Tonello et al., 2009; Moreno et al., 2010) or during transport may also have contributed to this change. Precipitation in Patagonian source regions is closely related to changes in surface wind speed on the Andes western slope with an opposing pattern between wind speed and precipitation on the eastern slope, due to increasing cyclonic activity and the presence of the mountains causing a rain shadow effect (Berman et al., 2012; Moreno et al., 2010; Garreaud, 2007). Precipitation trends in South America vary across regions north and south during the Holocene with icefields in Patagonia (47–48° S, 73.4° W) and Andes experiencing arid conditions during the early (9400–6300 cal yr BP) and late (2400–1600 cal yr BPP) Holocene, while regions in Southern Patagonia (∼ 50° S; ∼ 72° W) received increased precipitation during the mid-late Holocene (Fig. 5d and e; Glasser et al., 2004; Tonello et al., 2009; Moreno et al., 2010). However, both regions show increased in precipitation during the mid-Holocene (∼ 7000–> 3000 cal yr BP; Fig. 5d and e; Glasser et al., 2004; Tonello et al., 2009; Moreno et al., 2010; Bamonte et al., 2015). At lower latitudes (∼ 44° S), there was a relative increase in effective moisture during the Holocene (∼ 9500–4200 years BP; de Porras et al., 2014). We note that the CMIP6-PIMP4 output models suggest a broad increase in precipitation over most of South America, with disagreement in the models over the southern South America (Fig. 4a). Paleoproxy lake records (Fig. 5d) also support a progressive increase in precipitation throughout the Holocene suggesting southward migration of the SHWW belt (Tonello et al., 2009).

Reduced dust entrainment in the mid-latitudes may be a result of either increases in vegetation and/or a southward shift in the SHWW. Modelled and paleoproxy increases in precipitation are also observed with increases in *Nothofagus* compared to grassland vegetation cover (Fig. 5e; i.e., Moreno et al., 2010). The increase in vegetation cover and precipitation can reduce soil erosion and dust entrainment, while increasing dust fallout (i.e., Mahowald et al., 2005; Tegen and Schepanski, 2018). Therefore, the Holocene decrease in South Pole dust may not merely be related to a southward migration of the SHWW away from the dust sources, but also to a rise in precipitation resulting from this shift that also suppressed dust mobilization.

4.4 Antarctic ice sheet thinning and CPP increase

Previous studies have linked CPP variability with changes in air mass advection and/or activation of local dust sources (Delmonte et al., 2020; Koffman et al., 2014; Albani et al., 2012; Wegner et al., 2012; Aarons et al., 2017; Gabrielli et al., 2010). We explore the changes in the SPC14 CPP within the context of the coarse particle concentration. The coarse particle concentration has a similar trend throughout the Holocene as the total particle concentration (Fig. 1a and b), suggesting predominantly similar dynamics between coarse and total particle concentration change. However, because the CPP increases throughout the Holocene (Fig. 1c) there must be an additional forcing mechanism(s) acting upon the coarse particles.

The increase in SPC14 CPP begins ∼ 8000–6000 years BP (Figs. 1 and 5a) coinciding with the timing of glacial retreat and dust source exposure in lower-elevation regions of Antarctica between ∼ 7500–6000 years BP (Fig. 5h; Jones et al., 2020, 2015; Stutz et al., 2021; Stone et al., 2003; Johnson et al., 2014; Hein et al., 2016; Kawamata et al., 2020). For consistency, we recalibrate ^{10}Be surface exposure ages using production rates from Putnam et al. (2010) and Kaplan et al. (2011; Sect. S1 in the Supplement). Newly exposed source areas in the Weddell Sea sector are plausible origins of dust in SPC14 given prevailing low-level wind patterns (Lazzara et al., 2012; Winski et al., 2021; Clem et al., 2020). However, because the South Pole has multiple air sources, either moving into the East Antarctic plateau via in the Weddell Sea (Winski et al., 2021; Clem et al., 2020; Lazzara et al., 2012) or across West Antarctica (Nicolas and Bromwich, 2011), we interpret the changes in coarse particles to reflect broader scale Antarctic changes rather than to indicate activation of a specific local source (Figs. 2 and 3).

Holocene icesheet thinning, leading to exposure of Antarctic dust sources, is primarily related to (1) ocean warming (Jones et al., 2020; Stutz et al., 2021), (2) change in glacial flow patterns (Hein et al., 2016), and/or (3) reduced buttressing (Stutz et al., 2021). Strengthening and/or southward latitudinal shifts in the SHWW have been shown to increase surface upwelling of relatively warmer circumpolar deep wa-

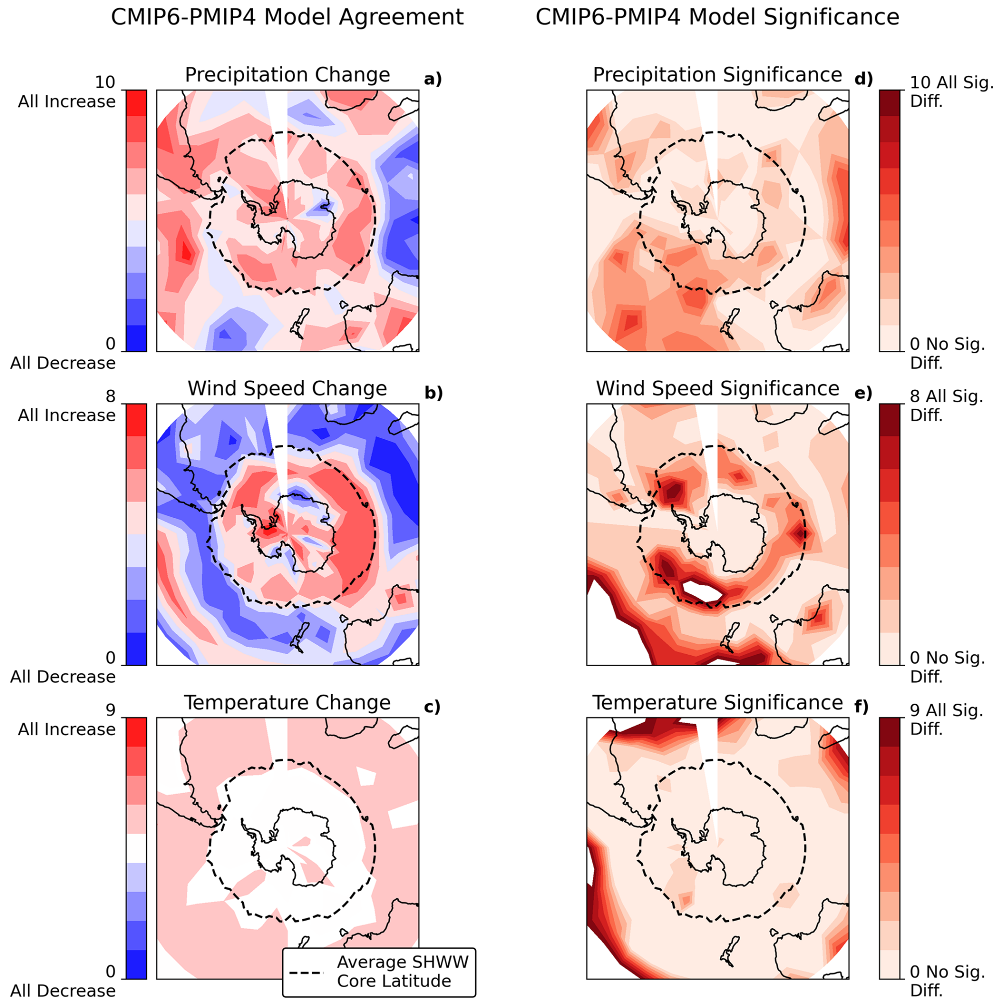

Figure 4. CMIP6-PMIP4 models agreement displaying difference between mid-Holocene and piControl precipitation **(a)**, wind speed **(b)**, and temperature **(c)**; Otto-Bliesner et al., 2017; Brierley et al., 2020). **(d)–(f)** highlights statistically significant difference (p-value < 0.05) between mid-Holocene and piControl using a two-sided t-test. Data are from a $10 \times 10^\circ$ grid to account for original model grid resolution (Table 1). **(a)–(c)** color bars indicate the number of models that infer a positive or no/negative change in each variable between 6000 years BP and during the Pre-Industrial. Red regions indicate a stronger model consensus towards an increase and blue indicates a consensus towards a decrease in the respective variable. Values in the middle represent a lack of consensus. **(d)–(f)** color bars highlight the number of models showing a significant change in the specific region, where darker red indicates all models used show a significant change. The black dotted line represents the average position of peak surface wind speed for both time periods.

ter (CDW) and increase air mass incursions driven by cyclogenesis into the Antarctic plateau (Hillenbrand et al., 2017; Carrasco et al., 2003). It seems likely that contracting, southward shifting, and accelerating SHWW, leading to warming ocean and atmosphere, is linked to the mid-Holocene glacial retreat (i.e., Albani et al., 2012; Koffman et al., 2014) and would increase Antarctic dust sources and the increase in CPP observed in SPC14. However, the coarse dust concentration has a slight decrease and a strong running correlation until ∼ 4000 years BP, suggesting a similar dust source and/or dynamics, which could indicate either (1) deflation of local Antarctic dust sources, similar to Holocene dynamics at Talos Dome (i.e., Albani et al., 2012) or (2) transport from mid-latitudinal sources (Adebiyi and Kok, 2020). Furthermore, the timing of surface elevation decrease around Antarctica corresponds to the SPC14 CPP increase, a southward shift in the Atlantic ITCZ, increasing rainfall in southern South America (Lago Guanaco), all of which can be explained by a southward shift in the SHWW due to increasing Southern Hemisphere temperatures (Fig. 5a, c, and e; Haug et al., 2001; Moreno et al., 2010; respectively). We suggest the CPP increase is primarily related to changes in remote dust contributions in the mid-latitudinal regions and also secondarily related to Antarctic dust source deflation.

A southward migration of the SHWW can simultaneously explain the decrease in South Pole dust concentration and

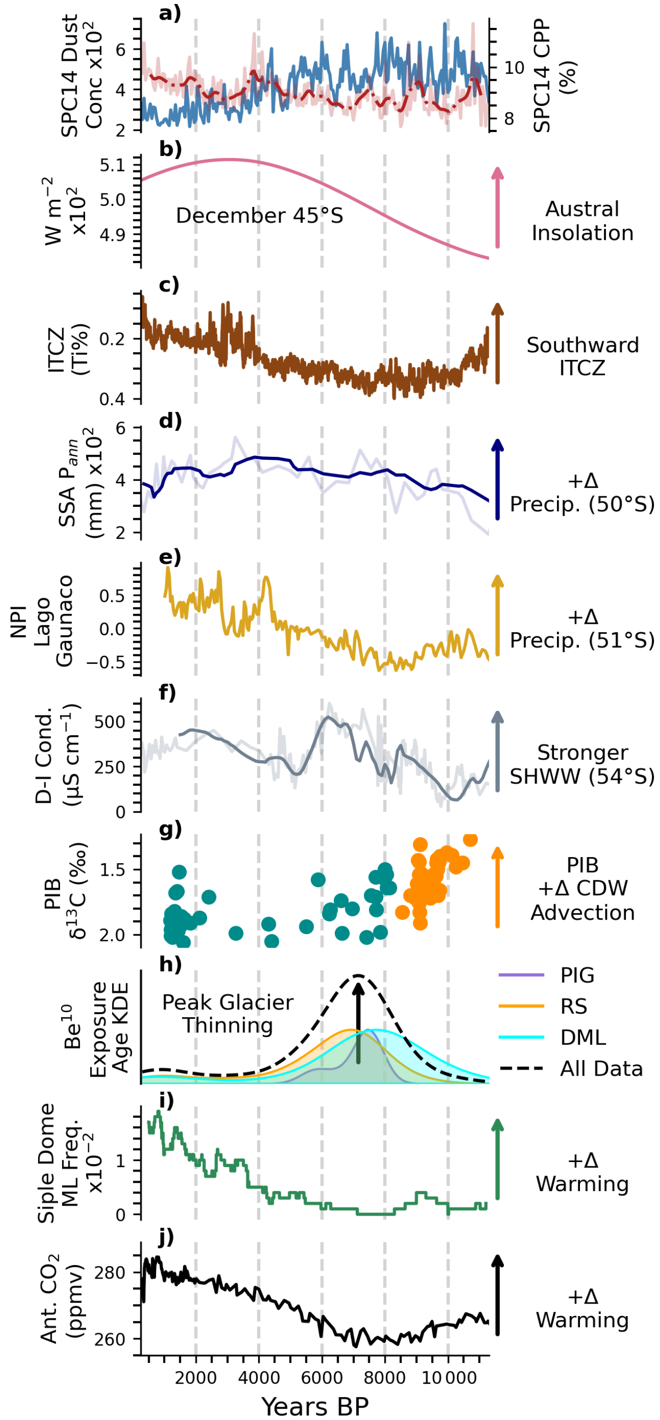

Figure 5. Southern Hemisphere perspective of climate variability (11300–250 years BP). **(a)–(j)** are stacks of different proxies spanning from the ITCZ to the South Pole. **(a)** is the SPC14 dust concentration (blue; # mL^{-1}) and CPP (light red shading) and CPP 11-point rolling mean (dashed red line; %). **(b)** summer (December) insolation at 45° S (Laskar et al., 2004), **(c)** Cariaco Basin Ti% (Haug et al., 2001), **(d)** Cerro Frias southern Patagonia precipitation reconstruction (Tonello et al., 2009), **(e)** Lago Guanaco precipitation reconstruction from Torres del Paine from 11 300 to 1000 years BP following Moreno et al. (2010), **(f)** Macquarie Island (South Pacific) diatom-inferred (D-I) conductivity measurements interpreted to reflect relative wind strength over the island (∼ 55° S; Saunders et al., 2018), **(g)** Pine Island Bay (PIB) δ^{13}C reflective of circumpolar deep water (CDW) advection (Hillenbrand et al., 2017), **(h)** ^{10}Be surface exposure from the Pine Island Glacier (Johnson et al., 2014), Ross Sea (Jones et al., 2020, 2015), and Dronning Maud Land (Kawamata et al., 2020). Scaling of each distribution kernel density estimate (KDE) is altered to show relative timing rather than magnitude of exposure dates, **(i)** Siple Dome melt layer frequency record (1000-year running mean; Das and Alley, 2008), and **(j)** compiled Antarctic CO_2 (Bereiter et al., 2015).

the increase in CPP, which is supported by our CMIP6-PMIP4 model trends and Southern Hemisphere proxy analysis. Southward migration of the SHWW is linked to Southern Ocean CO_2 outgassing (i.e., Moreno et al., 2010; Anderson et al., 2009; Toggweiler et al., 2006). The South Pole dust concentrations and CPP have significant relationships ($r = -0.76$ and 0.52, respectively, $p < 0.01$) with the composite Antarctic CO_2 record throughout the SPC14 Holocene record (Fig. 5j; Bereiter et al., 2015). However, based on our data, this is outside the scope of this paper.

We suggest that the southward migration of the SHWW was in-part driven by increases in Southern Hemisphere temperatures related to increasing insolation (Fig. 5b and i; Das and Alley, 2008; Laskar et al., 2004). Our SHWW model and proxy-based latitudinal reconstructions suggest that the latitudinal position and/or strength can reflect changes in regional temperature variability over millennial to centennial timescales consistent with previous studies (i.e., Jiang and Yan, 2020; Thompson and Solomon, 2002; Toggweiler et al., 2006). High-latitude zonally averaged Holocene temperature reconstructions (60–90° S latitude) differ, where Kaufman et al. (2020) identify a relatively stable Holocene temperature of $0.04 \pm 0.22 \Delta$ °C (slope $=< 0.01 \Delta$ °C kyr^{-1}; relative to pre-industrial temperature) and Osman et al. (2021) suggest a more insolation-like increase (slope $= 0.11 \Delta$ °C kyr^{-1}; relative to last two millennia). The insolation-like structure in the South Pole dust record seems most consistent with the reconstruction of Osman et al. (2021), suggesting progressive, insolation-style, Southern Hemisphere warming and corresponding southward shift in the SHWW.

5 Conclusions

Mid-to-high latitude Southern Hemisphere Holocene proxy records provide ample evidence for an orbitally-driven, progressive, southward shift of Holocene thermal gradients resulting in the strengthening of the SHWW beginning at the start of the Holocene with the most dynamic change occurring between 7000–3000 years BP. Together, the data suggest that high-southern latitude wind dynamics and resulting precipitation changes are driven by high-latitude hemispheric temperature change on orbital timescales. While there is broad agreement among many proxy records, the Pine Island Bay upwelling record shows a different pattern, with reduced wind-driven upwelling near West Antarctica after ∼ 8 ka (Fig. 5g; Hillenbrand et al., 2017). Zonal differences in wind strength may account for these apparently conflicting observations (Kaplan et al., 2016).

Opportunities for future research include describing the asymmetry in the timing of SHWW wind shifts between Western and Eastern Antarctica, which could influence the output of ocean derived CO_2 to the atmosphere. Our results further suggest the early Holocene may be a poor analogue for modern climate change. The SHWW southward shift and CO_2 transfer from the ocean to the atmosphere increased throughout the Holocene and has continued to increase today (Menviel et al., 2023). Identifying and examining WAIS stability within the context of Holocene changes therefore becomes critical if the early Holocene can no longer be used as an analogue to modern temperature change.

Data availability. Dust datasets and water isotope data used in this paper are available at the U.S. Antarctic Program Data Center (https://doi.org/10.15784/601553, Kreutz, 2022 and https://doi.org/10.15784/601239, Steig et al., 2020, respectively).

Supplement. The supplement related to this article is available online at https://doi.org/10.5194/cp-22-1741-2026-supplement.

Author contributions. AC analyzed the data and prepared the manuscript with contributions from all co-authors. KK, EO, JCD, and MW designed the experiments and guided the overall research effort. DF and ZT melted the core and measured the Abakus data and collected discrete samples. KA wrote the Abakus cleaning code. DW and BK provided data analysis and writing support. AP provided writing support. MH provided laboratory analysis feedback.

Competing interests. The contact author has declared that none of the authors has any competing interests.

Acknowledgements. This research was funded by the US National Science Foundation grants [1443336 (Osterberg); 1443397 (Kreutz); 1443663 (Cole-Dai); and 1443105, 1141839 (Steig)]. We thank Mark Twickler, Joseph Souney and the South Pole Ice Core (SPICEcore) Science Coordination Office for administering the project; the U.S. Ice Drilling Program for support activities through NSF Cooperative Agreement 1836328; the 109th New York Air National Guard for airlift in Antarctica; the field team who helped collect the core; the members of South Pole station who facilitated the field operations; the National Science Foundation Ice Core Facility for ice core processing; and the many student researchers involved in producing the data used in this research. The authors gratefully acknowledge the NOAA Air Resources Laboratory (ARL) for the provision of the HYSPLIT transport and dispersion model and/or READY website (https://www.ready.noaa.gov, last access: 5 January 2025) used in this publication. We acknowledge the World Climate Research Programme, which, through its Working Group on Coupled Modelling, coordinated and promoted CMIP6. We thank the climate modelling groups for producing and making available their model output, the Earth System Grid Federation (ESGF) for archiving the data and providing access, and the multiple funding agencies who support CMIP6 and ESGF. CMIP6 and PMIP4 model data was retrieved from the World Data Center for Climate (hosted by DKRZ) and Lawrence Livermore. We thank two anonymous reviewers, whose thoughtful suggestions and questions served to clarify and improve the paper.

Financial support. This research has been supported by the National Science Foundation (grant nos. 1443336, 1443397, 1443663, 1443105, and 1141839).

Review statement. This paper was edited by Barbara Stenni and reviewed by two anonymous referees.

References

Aarons, S. M., Aciego, S. M., Gabrielli, P., Delmonte, B., Koornneef, J. M., Wegner, A., and Blakowski, M. A.: The impact of glacier retreat from the Ross Sea on local climate: Characterization of mineral dust in the Taylor Dome ice core, East Antarctica, Earth Planet. Sci. Lett., 444, 34–44, https://doi.org/10.1016/j.epsl.2016.03.035, 2016.

Aarons, S. M., Aciego, S. M., Arendt, C. A., Blakowski, M. A., Steigmeyer, A., Gabrielli, P., Sierra-Hernández, M. R., Beaudon, E., Delmonte, B., Baccolo, G., May, N. W., and Pratt, K. A.: Dust composition changes from Taylor Glacier (East Antarctica) during the last glacial-interglacial transition: A multi-proxy approach, Quaternary Sci. Rev., 162, 60–71, https://doi.org/10.1016/j.quascirev.2017.03.011, 2017.

Aarons, S. M., Aciego, S. M., McConnell, J. R., Delmonte, B., and Baccolo, G.: Dust Transport to the Taylor Glacier, Antarctica, During the Last Interglacial, Geophys. Res. Lett., 46, 2261–2270, https://doi.org/10.1029/2018GL081887, 2019.

Adebiyi, A. A. and Kok, J. F.: Climate models miss most of the coarse dust in the atmosphere, Sci. Adv., 6, eaaz9507, https://doi.org/10.1126/sciadv.aaz9507, 2020.

Albani, S., Delmonte, B., Maggi, V., Baroni, C., Petit, J.-R., Stenni, B., Mazzola, C., and Frezzotti, M.: Interpreting last glacial to Holocene dust changes at Talos Dome (East Antarctica): implications for atmospheric variations from regional to hemispheric scales, Clim. Past, 8, 741–750, https://doi.org/10.5194/cp-8-741-2012, 2012.

Albani, S., Balkanski, Y., Mahowald, N., Winckler, G., Maggi, V., and Delmonte, B.: Aerosol-Climate Interactions During the Last Glacial Maximum, Curr. Clim. Change Rep., 4, 99–114, https://doi.org/10.1007/s40641-018-0100-7, 2018.

Anderson, R. F., Ali, S., Bradtmiller, L. I., Nielsen, S. H. H., Fleisher, M. Q., Anderson, B. E., and Burckle, L. H.: Wind-Driven Upwelling in the Southern Ocean and the Deglacial Rise in Atmospheric CO_2, Science, 323, 1443–1448, https://doi.org/10.1126/science.1167441, 2009.

Ardon-Dryer, K., Levin, Z., and Lawson, R. P.: Characteristics of immersion freezing nuclei at the South Pole station in Antarctica, Atmos. Chem. Phys., 11, 4015–4024, https://doi.org/10.5194/acp-11-4015-2011, 2011.

Arimoto, R., Zeng, T., Davis, D., Wang, Y., Khaing, H., Nesbit, C., and Huey, G.: Concentrations and sources of aerosol ions and trace elements during ANTCI-2003, Atmos. Environ., 42, 2864–2876, https://doi.org/10.1016/j.atmosenv.2007.05.054, 2008.

Baccolo, G., Cibin, G., Delmonte, B., Hampai, D., Marcelli, A., Di Stefano, E., Macis, S., and Maggi, V.: The Contribution of Synchrotron Light for the Characterization of Atmospheric Mineral Dust in Deep Ice Cores: Preliminary Results from the Talos Dome Ice Core (East Antarctica), Condensed Matter, 3, 25, https://doi.org/10.3390/condmat3030025, 2018.

Bamonte, F. P., Mancini, M. V., Sottile, G. D., Marcos, M. A., and Gogorza, C.: Vegetation dynamics from Lago San Martín area (Southwest Patagonia, Argentina) during the last 6,500 years, Veg. Hist. Archaeobot., 24, 267–277, https://doi.org/10.1007/s00334-014-0473-z, 2015.

Bereiter, B., Eggleston, S., Schmitt, J., Nehrbass-Ahles, C., Stocker, T. F., Fischer, H., Kipfstuhl, S., and Chappellaz, J.: Revision of the EPICA Dome C CO_2 record from 800 to 600 kyr before present, Geophys. Res. Lett., 42, 542–549, https://doi.org/10.1002/2014GL061957, 2015.

Berman, A. L., Silvestri, G., and Compagnucci, R.: Eastern Patagonia Seasonal Precipitation: Influence of Southern Hemisphere Circulation and Links with Subtropical South American Precipitation, J. Climate, 25, 6781–6795, https://doi.org/10.1175/JCLI-D-11-00514.1, 2012.

Bodhaine, B. A., Deluisi, J. J., Harris, J. M., Houmere, P., and Bauman, S.: Aerosol measurements at the South Pole, Tellus B, 38, 223–235, https://doi.org/10.3402/tellusb.v38i3-4.15131, 1986.

Breton, D. J., Koffman, B. G., Kurbatov, A. V., Kreutz, K. J., and Hamilton, G. S.: Quantifying Signal Dispersion in a Hybrid Ice Core Melting System, Environ. Sci. Technol., 46, 11922–11928, https://doi.org/10.1021/es302041k, 2012.

Brierley, C. M., Zhao, A., Harrison, S. P., Braconnot, P., Williams, C. J. R., Thornalley, D. J. R., Shi, X., Peterschmitt, J.-Y., Ohgaito, R., Kaufman, D. S., Kageyama, M., Hargreaves, J. C., Erb, M. P., Emile-Geay, J., D'Agostino, R., Chandan, D., Carré, M., Bartlein, P. J., Zheng, W., Zhang, Z., Zhang, Q., Yang, H., Volodin, E. M., Tomas, R. A., Routson, C., Peltier, W. R., Otto-Bliesner, B., Morozova, P. A., McKay, N. P., Lohmann, G., Legrande, A. N., Guo, C., Cao, J., Brady, E., Annan, J. D., and Abe-Ouchi, A.: Large-scale features and evaluation of the PMIP4-CMIP6 midHolocene simulations, Clim. Past, 16, 1847–1872, https://doi.org/10.5194/cp-16-1847-2020, 2020.

Bronselaer, B., Russell, J. L., Winton, M., Williams, N. L., Key, R. M., Dunne, J. P., Feely, R. A., Johnson, K. S., and Sarmiento, J. L.: Importance of wind and meltwater for observed chemical and physical changes in the Southern Ocean, Nat. Geosci., 13, 35–42, https://doi.org/10.1038/s41561-019-0502-8, 2020.

Carrasco, J. F., Bromwich, D. H., and Monaghan, A. J.: Distribution and Characteristics of Mesoscale Cyclones in the Antarctic: Ross Sea Eastward to the Weddell Sea, Mon. Weather Rev., 131, 289–301, https://doi.org/10.1175/1520-0493(2003)131<0289:dacomc>2.0.co;2, 2003.

Casey, K. A., Fudge, T. J., Neumann, T. A., Steig, E. J., and Cavitte, M. G. P.: The 1500 m South Pole ice core: recovering a 40 ka environmental record, Ann. Glaciol., 55, 137–146, https://doi.org/10.3189/2014AoG68A016, 2014.

Chesler, A., Winski, D., Kreutz, K., Koffman, B., Osterberg, E., Ferris, D., Thundercloud, Z., Mohan, J., Cole-Dai, J., Wells, M., Handley, M., Putnam, A., Anderson, K., and Harmon, N.: Non-spherical microparticle shape in Antarctica during the last glacial period affects dust volume-related metrics, Clim. Past, 19, 477–492, https://doi.org/10.5194/cp-19-477-2023, 2023.

Clem, K. R., Fogt, R. L., Turner, J., Lintner, B. R., Marshall, G. J., Miller, J. R., and Renwick, J. A.: Record warming at the South Pole during the past three decades, Nat. Clim. Change, 10, 762–770, https://doi.org/10.1038/s41558-020-0815-z, 2020.

Das, S. B. and Alley, R. B.: Rise in frequency of surface melting at Siple Dome through the Holocene: Evidence for increasing marine influence on the climate of West Antarctica, J. Geophys. Res.-Atmos., 113, https://doi.org/10.1029/2007JD008790, 2008.

Delmonte, B., Petit, J., and Maggi, V.: Glacial to Holocene implications of the new 27000-year dust record from the EPICA Dome C (East Antarctica) ice core, Clim. Dynam., 18, 647–660, https://doi.org/10.1007/s00382-001-0193-9, 2002.

Delmonte, B., Petit, J.-R., Krinner, G., Maggi, V., Jouzel, J., and Udisti, R.: Ice core evidence for secular variability and 200-year dipolar oscillations in atmospheric circulation over East Antarctica during the Holocene, Clim. Dynam., 24, 641–654, https://doi.org/10.1007/s00382-005-0012-9, 2005.

Delmonte, B., Baroni, C., Andersson, P. S., Narcisi, B., Salvatore, M. C., Petit, J. R., Scarchilli, C., Frezzotti, M., Albani, S., and Maggi, V.: Modern and Holocene aeolian dust variability from Talos Dome (Northern Victoria Land) to the interior of the Antarctic ice sheet, Quaternary Sci. Rev., 64, 76–89, https://doi.org/10.1016/j.quascirev.2012.11.033, 2013.

Delmonte, B., Winton, H., Baroni, M., Baccolo, G., Hansson, M., Andersson, P., Baroni, C., Salvatore, M. C., Lanci, L., and Maggi, V.: Holocene dust in East Antarctica: Provenance and variability in time and space, The Holocene, 30, 546–558, https://doi.org/10.1177/0959683619875188, 2020.

Denton, G. H., Putnam, A. E., Russell, J. L., Barrell, D. J. A., Schaefer, J. M., Kaplan, M. R., and Strand, P. D.: The Zealandia Switch: Ice age climate shifts viewed from Southern Hemisphere moraines, Quaternary Sci. Rev., 257, 106771, https://doi.org/10.1016/j.quascirev.2020.106771, 2021.

de Porras, M. E., Maldonado, A., Quintana, F. A., Martel-Cea, A., Reyes, O., and Méndez, C.: Environmental and climatic changes in central Chilean Patagonia since the Late Glacial (Mallín El Embudo, 44° S), Clim. Past, 10, 1063–1078, https://doi.org/10.5194/cp-10-1063-2014, 2014.

Dome Fuji Ice Core Project Members: Kawamura, K., Abe-Ouchi, A., Motoyama, H., Ageta, Y., Aoki, S., Azuma, N., Fujii, Y., Fujita, K., Fujita, S., Fukui, K., Furukawa, T., Furusaki, A., Goto-Azuma, K., Greve, R., Hirabayashi, M., Hondoh, T., Hori, A., Horikawa, S., Horiuchi, K., Igarashi, M., Iizuka, Y., Kameda, T., Kanda, H., Kohno, M., Kuramoto, T., Matsushi, Y., Miyahara, M., Miyake, T., Miyamoto, A., Nagashima, Y., Nakayama, Y., Nakazawa, T., Nakazawa, F., Nishio, F., Obinata, I., Ohgaito, R., Oka, A., Okuno, J. i., Okuyama, J., Oyabu, I., Parrenin, F., Pattyn, F., Saito, F., Saito, T., Saito, T., Sakurai, T., Sasa, K., Seddik, H., Shibata, Y., Shinbori, K., Suzuki, K., Suzuki, T., Takahashi, A., Takahashi, K., Takahashi, S., Takata, M., Tanaka, Y., Uemura, R., Watanabe, G., Watanabe, O., Yamasaki, T., Yokoyama, K., Yoshimori, M., and Yoshimoto, T.: State dependence of climatic instability over the past 720,000 years from Antarctic ice cores and climate modeling, Sci. Adv., 3, e1600446, https://doi.org/10.1126/sciadv.1600446, 2017.

Fujii, Y., Kohno, M., Matoba, S., Motoyama, H., and Watanabe, O.: A 320 k-year record of microparticles in the Dome Fuji, Antarctica ice core measured by laser-light scattering, Mem. Natl. Inst. Polar Res. Spec. Issue, 57, 46–62, 2003.

Gabrielli, P., Wegner, A., Petit, J. R., Delmonte, B., and De Deckker, P.: A major glacial-interglacial change in aeolian dust composition inferred from Rare Earth Elements in Antarctic ice, Quaternary Sci. Rev., 29, 265–273, https://doi.org/10.1016/j.quascirev.2009.09.002, 2010.

Garreaud, R.: Precipitation and Circulation Covariability in the Extratropics, J. Climate, 20, 4789–4797, https://doi.org/10.1175/JCLI4257.1, 2007.

Glasser, N. F., Harrison, S., Winchester, V., and Aniya, M.: Late Pleistocene and Holocene palaeoclimate and glacier fluctuations in Patagonia, Global Planet. Change, 43, 79–101, https://doi.org/10.1016/j.gloplacha.2004.03.002, 2004.

Harris, J. M.: An analysis of 5-day midtropospheric flow patterns for the South Pole: 1985–1989, Tellus B, https://doi.org/10.3402/tellusb.v44i4.15466, 1992.

Haug, G. H., Hughen, K. A., Sigman, D. M., Peterson, L. C., and Röhl, U.: Southward Migration of the Intertropical Convergence Zone Through the Holocene, Science, 293, 1304–1308, https://doi.org/10.1126/science.1059725, 2001.

Hein, A. S., Marrero, S. M., Woodward, J., Dunning, S. A., Winter, K., Westoby, M. J., Freeman, S. P. H. T., Shanks, R. P., and Sugden, D. E.: Mid-Holocene pulse of thinning in the Weddell Sea sector of the West Antarctic ice sheet, Nat. Commun., 7, 12511, https://doi.org/10.1038/ncomms12511, 2016.

Hillenbrand, C.-D., Smith, J. A., Hodell, D. A., Greaves, M., Poole, C. R., Kender, S., Williams, M., Andersen, T. J., Jernas, P. E., Elderfield, H., Klages, J. P., Roberts, S. J., Gohl, K., Larter, R. D., and Kuhn, G.: West Antarctic Ice Sheet retreat driven by Holocene warm water incursions, Nature, 547, 43–48, https://doi.org/10.1038/nature22995, 2017.

Hogan, A., Kebschull, K., Townsend, R., Murphey, B., Samson, J., and Barnard, S.: Particle concentrations at the South Pole, on meteorological and climatological time scales; Is the difference important?, Geophys. Res. Lett., 11, 850–853, https://doi.org/10.1029/GL011i009p00850, 1984.

Jiang, N. X. and Yan, Q.: Evolution of the meridional shift of the subtropical and subpolar westerly jet over the Southern Hemisphere during the past 21,000 years, Quaternary Sci. Rev., 246, 10.1016/j.quascirev.2020.106544, 2020.

Johnson, J. S., Bentley, M. J., Smith, J. A., Finkel, R. C., Rood, D. H., Gohl, K., Balco, G., Larter, R. D., and Schaefer, J. M.: Rapid Thinning of Pine Island Glacier in the Early Holocene, Science, 343, 999–1001, https://doi.org/10.1126/science.1247385, 2014.

Jones, R. S., Mackintosh, A. N., Norton, K. P., Golledge, N. R., Fogwill, C. J., Kubik, P. W., Christl, M., and Greenwood, S. L.: Rapid Holocene thinning of an East Antarctic outlet glacier driven by marine ice sheet instability, Nat. Commun., 6, 8910, https://doi.org/10.1038/ncomms9910, 2015.

Jones, R. S., Whitmore, R. J., Mackintosh, A. N., Norton, K. P., Eaves, S. R., Stutz, J., and Christl, M.: Regional-scale abrupt Mid-Holocene ice sheet thinning in the western Ross Sea, Antarctica, Geology, 49, 278–282, https://doi.org/10.1130/g48347.1, 2020.

Kaplan, M. R., Strelin, J. A., Schaefer, J. M., Denton, G. H., Finkel, R. C., Schwartz, R., Putnam, A. E., Vandergoes, M. J., Goehring, B. M., and Travis, S. G.: In-situ cosmogenic ^{10}Be production rate at Lago Argentino, Patagonia: Implications for late-glacial climate chronology, Earth Planet. Sci. Lett., 309, 21–32, https://doi.org/10.1016/j.epsl.2011.06.018, 2011.

Kaplan, M. R., Schaefer, J. M., Strelin, J. A., Denton, G. H., and Anderson, R. F.: Patagonian and southern South Atlantic view of Holocene climate, Quaternary Sci. Rev., 141, 112–125, https://doi.org/10.1016/j.quascirev.2016.03.014, 2016.

Kaufman, D., McKay, N., Routson, C., Erb, M., Dätwyler, C., Sommer, P. S., Heiri, O., and Davis, B.: Holocene global mean surface temperature, a multi-method reconstruction approach, Sci. Data, 7, 201, https://doi.org/10.1038/s41597-020-0530-7, 2020.

Kawamata, M., Suganuma, Y., Doi, K., Misawa, K., Hirabayashi, M., Hattori, A., and Sawagaki, T.: Abrupt Holocene ice-sheet thinning along the southern Soya Coast, Lützow-Holm Bay, East Antarctica, revealed by glacial geomorphology and surface exposure dating, Quaternary Sci. Rev., 247, 106540, https://doi.org/10.1016/j.quascirev.2020.106540, 2020.

Koffman, B. and Kreutz, K.: Evidence that local dust sources supply low-elevation Antarctic regions, PAGES Magazine, 22, 76–77, 2014.

Koffman, B. G., Kreutz, K. J., Breton, D. J., Kane, E. J., Winski, D. A., Birkel, S. D., Kurbatov, A. V., and Handley, M. J.: Centennial-scale variability of the Southern Hemisphere westerly wind belt in the eastern Pacific over the past two millennia, Clim. Past, 10, 1125–1144, https://doi.org/10.5194/cp-10-1125-2014, 2014.

Koffman, B. G., Goldstein, S. L., Winckler, G., Kaplan, M. R., Bolge, L., and Biscaye, P.: Abrupt Changes in Atmospheric Circulation During the Medieval Climate Anomaly and Little Ice Age Recorded by Sr-Nd Isotopes in the Siple Dome Ice Core, Antarct. Paleoceanogr. Paleoclimatol., 38, e2022PA004543, https://doi.org/10.1029/2022PA004543, 2023.

Kreutz, K.: "South Pole (SPC14) microparticle concentration, mass concentration, flux, particle-size-distribution mode, and aspect ratio measurements" U.S. Antarctic Program (USAP) Data Center [data set], https://doi.org/10.15784/601553, 2022.

Lambert, F., Delmonte, B., Petit, J. R., Bigler, M., and Kaufmann, P. R.: Dust-climate couplings over the past 800,000 years from the EPICA Dome C ice core, Nature (London), 452, 616–619, https://doi.org/10.1038/nature06763, 2008.

Lambert, F., Bigler, M., Steffensen, J. P., Hutterli, M., and Fischer, H.: Centennial mineral dust variability in high-resolution ice core data from Dome C, Antarctica, Clim. Past, 8, 609–623, https://doi.org/10.5194/cp-8-609-2012, 2012.

Lamy, F., Kilian, R., Arz, H. W., Francois, J.-P., Kaiser, J., Prange, M., and Steinke, T.: Holocene changes in the position and intensity of the southern westerly wind belt, Nat. Geosci., 3, 695–699, https://doi.org/10.1038/ngeo959, 2010.

Laskar, J., Robutel, P., Joutel, F., Gastineau, M., Correia, A. C. M., and Levrard, B.: A long-term numerical solution for the insolation quantities of the Earth, A&A, 428, 261–285, https://doi.org/10.1051/0004-6361:20041335, 2004.

Lazzara, M. A., Keller, L. M., Markle, T., and Gallagher, J.: Fifty-year Amundsen–Scott South Pole station surface climatology, Atmos. Res., 118, 240–259, https://doi.org/10.1016/j.atmosres.2012.06.027, 2012.

Mahowald, N. M., Baker, A. R., Bergametti, G., Brooks, N., Duce, R. A., Jickells, T. D., Kubilay, N., Prospero, J. M., and Tegen, I.: Atmospheric global dust cycle and iron inputs to the ocean, Global Biogeochem. Cy., 19, https://doi.org/10.1029/2004GB002402, 2005.

Marcott, S. A., Shakun, J. D., Clark, P. U., and Mix, A. C.: A Reconstruction of Regional and Global Temperature for the Past 11,300 Years, Science, 339, 1198–1201, https://doi.org/10.1126/science.1228026, 2013.

Markle, B. R., Steig, E. J., Roe, G. H., Winckler, G., and McConnell, J. R.: Concomitant variability in high-latitude aerosols, water isotopes and the hydrologic cycle, Nat. Geosci., 11, 853–859, https://doi.org/10.1038/s41561-018-0210-9, 2018.

McConnell, J. R., Aristarain, A. J., Banta, J. R., Edwards, P. R., and Simões, J. C.: 20th-Century doubling in dust archived in an Antarctic Peninsula ice core parallels climate change and desertification in South America, P. Natl. Acad. Sci. USA, 104, 5743–5748, https://doi.org/10.1073/pnas.0607657104, 2007.

Menviel, L. C., Spence, P., Kiss, A. E., Chamberlain, M. A., Hayashida, H., England, M. H., and Waugh, D.: Enhanced Southern Ocean CO_2 outgassing as a result of stronger and poleward shifted southern hemispheric westerlies, Biogeosciences, 20, 4413–4431, https://doi.org/10.5194/bg-20-4413-2023, 2023.

Moreno, P. I., Francois, J. P., Moy, C. M., and Villa-Martínez, R.: Covariability of the Southern Westerlies and atmospheric CO_2 during the Holocene, Geology, 38, 727–730, https://doi.org/10.1130/g30962.1, 2010.

Mulvaney, R., Abram, N. J., Hindmarsh, R. C. A., Arrowsmith, C., and Fleet, L.: Recent Antarctic Peninsula warming relative to Holocene climate and ice-shelf history, Nature (London), 489, 141–144, https://doi.org/10.1038/nature11391, 2012.

Nicolas, J. P. and Bromwich, D. H.: Climate of West Antarctica and Influence of Marine Air Intrusions, J. Climate, 24, 49–67, https://doi.org/10.1175/2010jcli3522.1, 2011.

Osman, M. B., Tierney, J. E., Zhu, J., Tardif, R., Hakim, G. J., King, J., and Poulsen, C. J.: Globally resolved surface temperatures since the Last Glacial Maximum, Nature, 599, 239–244, https://doi.org/10.1038/s41586-021-03984-4, 2021.

Osterberg, E. C., Handley, M. J., Sneed, S. B., Mayewski, P. A., and Kreutz, K. J.: Continuous ice core melter system with discrete sampling for major ion, trace element, and stable isotope analyses, Environ. Sci. Technol., 40, 3355–3361, https://doi.org/10.1021/es052536w, 2006.

Otto-Bliesner, B. L., Braconnot, P., Harrison, S. P., Lunt, D. J., Abe-Ouchi, A., Albani, S., Bartlein, P. J., Capron, E., Carlson, A. E., Dutton, A., Fischer, H., Goelzer, H., Govin, A., Haywood, A., Joos, F., LeGrande, A. N., Lipscomb, W. H., Lohmann, G., Mahowald, N., Nehrbass-Ahles, C., Pausata, F. S. R., Peterschmitt, J.-Y., Phipps, S. J., Renssen, H., and Zhang, Q.: The PMIP4 contribution to CMIP6 – Part 2: Two interglacials, scientific objective and experimental design for Holocene and Last Interglacial simulations, Geosci. Model Dev., 10, 3979–4003, https://doi.org/10.5194/gmd-10-3979-2017, 2017.

Parungo, F., Bodhaine, B., and Bortniak, J.: Seasonal variation in antarctic aerosol, J. Aerosol Sci., 12, 491–504, https://doi.org/10.1016/0021-8502(81)90052-5, 1981.

Perren, B. B., Hodgson, D. A., Roberts, S. J., Sime, L., Van Nieuwenhuyze, W., Verleyen, E., and Vyverman, W.: Southward migration of the Southern Hemisphere westerly winds corresponds with warming climate over centennial timescales, Commun. Earth Environ., 1, 58, https://doi.org/10.1038/s43247-020-00059-6, 2020.

Petit, J. R., Mourner, L., Jouzel, J., Korotkevich, Y. S., Kotlyakov, V. I., and Lorius, C.: Palaeoclimatological and chronological implications of the Vostok core dust record, Nature, 343, 56–58, 1990.

Potenza, M. A. C., Albani, S., Delmonte, B., Villa, S., Sanvito, T., Paroli, B., Pullia, A., Baccolo, G., Mahowald, N., and Maggi, V.: Shape and size constraints on dust optical properties from the Dome C ice core, Antarctica, Sci. Rep., 6, 9, https://doi.org/10.1038/srep28162, 2016.

Putnam, A. E., Schaefer, J. M., Barrell, D. J. A., Vandergoes, M., Denton, G. H., Kaplan, M. R., Finkel, R. C., Schwartz, R., Goehring, B. M., and Kelley, S. E.: In situ cosmogenic ^{10}Be production-rate calibration from the Southern Alps, New Zealand, Quaternary Geochronol., 5, 392–409, https://doi.org/10.1016/j.quageo.2009.12.001, 2010.

Putnam, A. E., Schaefer, J. M., Denton, G. H., Barrell, D. J. A., Finkel, R. C., Andersen, B. G., Schwartz, R., Chinn, T. J. H., and Doughty, A. M.: Regional climate control of glaciers in New Zealand and Europe during the pre-industrial Holocene, Nat. Geosci., 5, 627–630, https://doi.org/10.1038/ngeo1548, 2012.

Rolph, G., Stein, A., and Stunder, B.: Real-time Environmental Applications and Display sYstem: READY, Environ. Modell. Softw., 95, 210–228, https://doi.org/10.1016/j.envsoft.2017.06.025, 2017.

Russell, J. L., Dixon, K. W., Gnanadesikan, A., Stouffer, R. J., and Toggweiler, J. R.: The Southern Hemisphere Westerlies in a Warming World: Propping Open the Door to the Deep Ocean, J. Climate, 19, 6382–6390, https://doi.org/10.1175/jcli3984.1, 2006.

Saunders, K. M., Roberts, S. J., Perren, B., Butz, C., Sime, L., Davies, S., Van Nieuwenhuyze, W., Grosjean, M., and Hodgson, D. A.: Holocene dynamics of the Southern Hemisphere westerly winds and possible links to CO_2 outgassing, Nat. Geosci., 11, 650–655, https://doi.org/10.1038/s41561-018-0186-5, 2018.

Schwanck, F., Simões, J. C., Handley, M., Mayewski, P. A., Auger, J. D., Bernardo, R. T., and Aquino, F. E.: A 125-year record of climate and chemistry variability at the Pine Island Glacier ice divide, Antarctica, The Cryosphere, 11, 1537–1552, https://doi.org/10.5194/tc-11-1537-2017, 2017.

Sheridan, P., Andrews, E., Schmeisser, L., Vasel, B., and Ogren, J.: Aerosol Measurements at South Pole: Climatology and Impact of Local Contamination, Aerosol Air Qual. Res., 16, 855–872, https://doi.org/10.4209/aaqr.2015.05.0358, 2016.

Simonsen, M. F., Cremonesi, L., Baccolo, G., Bosch, S., Delmonte, B., Erhardt, T., Kjær, H. A., Potenza, M., Svensson, A., and Vallelonga, P.: Particle shape accounts for instrumental discrepancy in ice core dust size distributions, Clim. Past, 14, 601–608, https://doi.org/10.5194/cp-14-601-2018, 2018.

Steig, E. J., Jones, T. R., Kahle, E., Morris, V., Schauer, A., Vaughn, B., and White, J.: "South Pole high resolution ice core water stable isotope record for dD, d^{18}O", U.S. Antarctic Program (USAP) Data Center [data set], https://doi.org/10.15784/601239, 2020.

Steig, E. J., Jones, T. R., Schauer, A. J., Kahle, E. C., Morris, V. A., Vaughn, B. H., Davidge, L., and White, J. W. C.: Continuous-Flow Analysis of δ^{17}O, δ^{18}O, and δD of H_2O on an Ice Core from the South Pole, Front. Earth Sci., 9, https://doi.org/10.3389/feart.2021.640292, 2021.

Stein, A. F., Draxler, R. R., Rolph, G. D., Stunder, B. J. B., Cohen, M. D., and Ngan, F.: NOAA's HYSPLIT Atmospheric Transport and Dispersion Modeling System, B. Am. Meteorol. Soc., 96, 2059–2077, https://doi.org/10.1175/BAMS-D-14-00110.1, 2015.

Stone, J. O., Balco, G. A., Sugden, D. E., Caffee, M. W., Sass, L. C., Cowdery, S. G., and Siddoway, C.: Holocene Deglaciation of Marie Byrd Land, West Antarctica, Science, 299, 99–102, 2003.

Stutz, J., Mackintosh, A., Norton, K., Whitmore, R., Baroni, C., Jamieson, S. S. R., Jones, R. S., Balco, G., Salvatore, M. C., Casale, S., Lee, J. I., Seong, Y. B., McKay, R., Vargo, L. J., Lowry, D., Spector, P., Christl, M., Ivy Ochs, S., Di Nicola, L., Iarossi, M., Stuart, F., and Woodruff, T.: Mid-Holocene thinning of David Glacier, Antarctica: chronology and controls, The Cryosphere, 15, 5447–5471, https://doi.org/10.5194/tc-15-5447-2021, 2021.

Sugden, D. E., McCulloch, R. D., Bory, A. J. M., and Hein, A. S.: Influence of Patagonian glaciers on Antarctic dust deposition during the last glacial period, Nat. Geosci., 2, 281–285, https://doi.org/10.1038/ngeo474, 2009.

Tegen, I. and Schepanski, K.: Climate Feedback on Aerosol Emission and Atmospheric Concentrations, Curr. Clim. Change Rep., 4, 1–10, https://doi.org/10.1007/s40641-018-0086-1, 2018.

Thompson, D. W. J. and Solomon, S.: Interpretation of Recent Southern Hemisphere Climate Change, Science, 296, 895–899, https://doi.org/10.1126/science.1069270, 2002.

Toggweiler, J. R. and Russell, J.: Ocean circulation in a warming climate, Nature, 451, 286–288, 2008.

Toggweiler, J. R., Russell, J. L., and Carson, S.: Midlatitude westerlies, atmospheric CO_2, and climate change during the ice ages, Paleoceanography, 21, https://doi.org/10.1029/2005PA001154, 2006.

Tonello, M. S., Mancini, M. V., and Seppä, H.: Quantitative reconstruction of Holocene precipitation changes in southern Patagonia, Quaternary Res., 72, 410–420, https://doi.org/10.1016/j.yqres.2009.06.011, 2009.

Tuncel, G., Aras, N. K., and Zoller, W. H.: Temporal variations and sources of elements in the South Pole atmosphere: 1. Nonenriched and moderately enriched elements, J. Geophys. Res.-Atmos., 94, 13025–13038, https://doi.org/10.1029/JD094iD10p13025, 1989.

Vecchio, M. A., Costas-Rodríguez, M., Caiazzo, L., Bruschi, F., Hobin, K., Vanhaecke, F., and Grotti, M.: Provenance of mineral dust deposited on Antarctica over the last sixty years by strontium isotopic analysis of snow from Dome C, Atmos. Environ., 338, 120850, https://doi.org/10.1016/j.atmosenv.2024.120850, 2024.

Wegner, A., Gabrielli, P., Wilhelms-Dick, D., Ruth, U., Kriews, M., De Deckker, P., Barbante, C., Cozzi, G., Delmonte, B., and Fischer, H.: Change in dust variability in the Atlantic sector of Antarctica at the end of the last deglaciation, Clim. Past, 8, 135–147, https://doi.org/10.5194/cp-8-135-2012, 2012.

Winski, D. A., Fudge, T. J., Ferris, D. G., Osterberg, E. C., Fegyveresi, J. M., Cole-Dai, J., Thundercloud, Z., Cox, T. S., Kreutz, K. J., Ortman, N., Buizert, C., Epifanio, J., Brook, E. J., Beaudette, R., Severinghaus, J., Sowers, T., Steig, E. J., Kahle, E. C., Jones, T. R., Morris, V., Aydin, M., Nicewonger, M. R., Casey, K. A., Alley, R. B., Waddington, E. D., Iverson, N. A., Dunbar, N. W., Bay, R. C., Souney, J. M., Sigl, M., and McConnell, J. R.: The SP19 chronology for the South Pole Ice Core – Part 1: volcanic matching and annual layer counting, Clim. Past, 15, 1793–1808, https://doi.org/10.5194/cp-15-1793-2019, 2019.

Winski, D. A., Osterberg, E. C., Kreutz, K. J., Ferris, D. G., Cole-Dai, J., Thundercloud, Z., Huang, J., Alexander, B., Jaeglé, L., Kennedy, J. A., Larrick, C., Kahle, E. C., Steig, E. J., and Jones, T. R.: Seasonally Resolved Holocene Sea Ice Variability Inferred From South Pole Ice Core Chemistry, Geophys. Res. Lett., 48, e2020GL091602, https://doi.org/10.1029/2020GL091602, 2021.

Zwier, M., van der Bilt, W. G., de Stigter, H., and Bjune, A. E.: Pollen evidence of variations in Holocene climate and Southern Hemisphere Westerly Wind strength on sub-Antarctic South Georgia, The Holocene, 32, 147–158, https://doi.org/10.1177/09596836211060495, 2022.